Automatic λ-Control with Offset Compensation in DFB Intradyne Receiver for udWDM-PON

Jeison Tabares, Victor Polo, Iván Cano, and Josep Prat, *Member, IEEE*

***Abstract*—A complete automatic wavelength control (AWC) for digital coherent receivers which performs local laser tuning and feed-forward frequency offset compensation is presented. We demonstrate the feasibility of the concept in a 1.25Gbps DPSK intradyne system, achieving accurate performance with common DFB lasers for cost-efficient optical access networks.**

***Index Terms*—Coherent detection, differential phase shift keying (DPSK), digital signal processing (DSP), frequency estimation, wavelength tuning.**

I. Introduction

IMPLEMENTATION of digital signal processing (DSP) techniques to coherent receivers has enabled transmission of spectrally-efficient advanced modulation formats and effective impairments compensation. A major challenge in coherent detection is the synchronization of the optical carrier. To avoid the employment of phase-locked-loop systems, homodyne phase-diversity architectures also known as intradyne receivers can operate with free-running local oscillator (LO) lasers overcoming synchronization problems and additional impairments by further processing of In-phase (I) and Quadrature (Q) baseband signals [1]. In this phase-diversity scheme the optical frequency of transmitter (Tx) and LO lasers must remain as close as possible to each other to avoid penalty at detection. Typical DFB lasers implemented for cost-efficient solutions exhibit high wavelength variability due to environmental changes and frequency accuracy of ±2.5GHz over lifetime [2], becoming a major issue in ultra-dense wavelength division multiplexing passive optical networks (udWDM-PON), that implements the wavelength-to-the-user concept by allocating hundreds of wavelengths in dense spectral distribution as narrow as 6.25GHz spacing between adjacent channels running at 1.25Gbps, providing high aggregate capacity to the PON [3].

Manuscript received September 18, 2014. (Write the date on which you submitted your paper for review.) This work was supported in part by the European Projects COCONUT and ROMULA, and the FPU program from Education Ministry of Spain.

The authors are with the Universitat Politècnica de Catalunya, Teoria del Senyal i Comunicacions, Barcelona E-08034, Spain (e-mail: jtabares@tsc.upc.edu; polo@tsc.upc.edu; ivan.cano@tsc.upc.edu; jprat@tsc.upc.edu).

Previous works have demonstrated frequency offset correction by either feed-back or feed-forward techniques, with a frequency range up to half the symbol-rate drift, operating at laser linewidth-symbol time product $\Delta\upsilon T_b < 3\cdot10^{-5}$ [2], [4], [5]. Alternative strategies have been also proposed like remote wavelength control by a centralized wavelength locker [6]. In this paper, we develop, for the first time to the best of our knowledge, an automatic wavelength control (AWC) in a DFB-based coherent intradyne DPSK receiver for udWDM systems, applying feed-forward tracking and feed-back stabilization. This dual strategy, performed by the same digital estimator block, improves the receiver performance avoiding the need of extra hardware for the feed-back tuning. Results show a real-time correction of ±500MHz frequency drift within 2dB maximum power penalty, at a sensitivity point of -47.5dBm received optical power for target BER = 10^{-4}.

The paper is organized as follows. Section II presents the general receiver architecture with the AWC. The frequency estimation and offset correction algorithms are introduced in sections III and IV, respectively. The experimental setup is described in section V, followed by the results which include frequency noise characterization and transmission tests.

II. Receiver Architecture

At the coherent intradyne receiver front-end, the incoming optical signal beats with the LO laser in an optical hybrid to provide phase-diversity operation, which combined with differential demodulation, overcome the phase noise effect that produces BER degradation. After photodetection, A/D conversion provides digital samples of the baseband signal to be processed at the DSP stage, which comprises frequency offset estimation, LO tuning, signal phase correction and data recovery, as depicted in Fig.1. In the DSP unit, frequency offset estimation and correction is performed prior demodulation and data recovery. The estimated offset enables

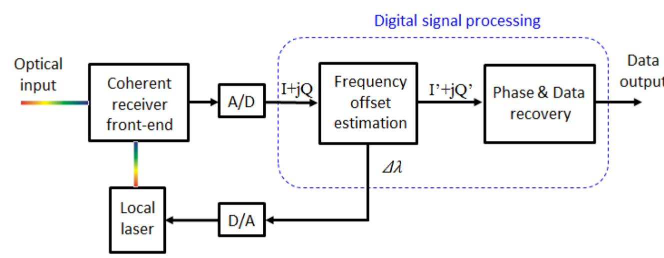

Fig. 1. Digital coherent receiver with AWC.

both feed-forward IQ data correction and feed-back loop towards LO for tuning. Afterwards, corrected IQ data are differentially demodulated by comparing the phase variation of each bit against the previous bit to extract the phase-encoded data. Finally, auto-correlation of the baseband signal is applied to decide the optimal sample period for clock recovery and data decision.

III. Frequency Estimation

The goal of the frequency estimation algorithm is to estimate the phase drift $\Delta\varphi = 2\pi\Delta f T_S$ between consecutive samples of the IQ signal, produced by the frequency mismatch $\Delta f = f_S - f_{LO}$ among transmitter (f_S) and LO (f_{LO}) optical frequencies, being T_S the sample time.

If the PSK modulation is removed from the baseband detected signal, the phase drift caused by laser phase noise can be considered constant over a number of consecutive samples, whereas the one caused by frequency drift changes a fixed value every sample time T_S. Therefore, blocks of digital samples from I+*j*Q signal are processed to obtain $\Delta\varphi$.

We evaluate two different algorithms from the variety of available algorithms used in signal processing for optical communications. One approach based on the Viterbi estimation model, and other based on the correlation of IQ components. These algorithms were selected due to its convenient implementation in DSP units, achieving good performance with relatively simple design [7]. For next discussions, let's consider the sampled detected complex signal

$$V_S[k] = I_k + jQ_k \quad (1)$$

A. Viterbi estimator

The first approach consists of a phase increment estimation algorithm based on Viterbi estimation model, which can be implemented as an angle-doubling algorithm for DPSK signals [4]. To estimate the phase drift, each sample of IQ signal is multiplied by the complex conjugate of the previous sample. Then, binary-PSK modulation is eliminated by taking the square power of the complex values. Finally $\Delta\varphi$ is extracted and averaged over the number of block samples, being expressed as

$$\Delta\varphi = \left\langle \arg\left\{ \left(V_S[k] V_S^*[k-1] \right)^2 \right\} \right\rangle \quad (2)$$

B. IQ correlation estimator

This scheme appears from the cross-product algorithms for frequency estimation and aims to extract the phase drift $\Delta\varphi$ from the correlation between IQ components [2]. In this regard, the cross-product of the complex signals $V_S[k]$ and its delayed version $V_S[k\text{-}1]$ are performed and then subtracted and averaged over the number of block samples, to obtain the imaginary part of the correlation function of IQ signal. Hence, calculation of $\Delta\varphi$ is related to the expression

$$\Delta\varphi \propto \left\langle I_{k-1} Q_k - I_k Q_{k-1} \right\rangle \quad (3)$$

IV. Frequency Offset Correction

The obtained phase drift $\Delta\varphi$ is able to drive either a feed-back loop for LO tuning and feed-forward phase offset compensation. Regarding to the feed-back loop, the estimated offset can be used as a feed-back metric for LO laser wavelength control, as proposed in [8]. On the other hand, for simultaneous feed-forward IQ offset compensation, the accumulated phase offset $k\Delta\varphi$, where k is the symbol index, must be corrected from each I+*j*Q sample to compensate the

$$I_k^{'} + jQ_k^{'} = (I_k + jQ_k)e^{-jk\Delta\varphi} \quad (4)$$

rotation of the constellation points in the complex plane. Afterwards, demodulation and data recovery is performed, as depicted in Fig.1.

V. Experimental Setup

The system was tested with a 2^7-1 NRZ-PRBS differentially encoded pattern of 2^{18} bits total length, stored in an arbitrary waveform generator (AWG) running at 1.25Gbps. The signal was used to directly phase-modulate an equalized and temperature-stabilized DFB laser with 4MHz linewidth to obtain a DPSK modulation [9]. A variable optical attenuator was placed to adjust the received optical power, as shown in Fig. 2.

At the receiver side, a 3x3 coupler as a 120º optical hybrid mixes incoming DPSK signal with LO laser, that is another 4MHz linewidth DFB laser with integrated electronic circuit for current and temperature control, emitting at 0dBm. Polarization state of Tx and LO was manually controlled to be matched. The use of the less complex 3x3 coupler provides the advantage of phase-diversity operation with only 3-photodiodes compared to the well-known 90º hybrid 4-photodiodes phase-diversity scheme.

After photodetection the three baseband electrical signals are A/D converted by a 50GSa/s real-time oscilloscope operating as a DSP unit. First, low-pass digital filtering at $0.65R_b$ cut-off frequency is applied for noise suppression and subsequently the three signals are adequately combined to obtain the IQ components [10]. A block length of 50 symbols was chosen for frequency offset estimation. Differential detection of both IQ signals was performed and then combined to counteract the laser phase noise effect. Finally, the bit error ratio (BER) was calculated by direct error counting on the received data.

At the feed-back loop, the estimated offset $\Delta\varphi$ is delivered to a digital proportional-integral (PI) controller previously adjusted by Ziegler-Nichols method to adequate the control signal to the dynamic response of the tunable LO laser. Next, a 400kHz I^2C digital interface via USB port drives the D/A conversion towards the LO control. The thermally tunable DFB laser used as LO implements an electronic fast frequency

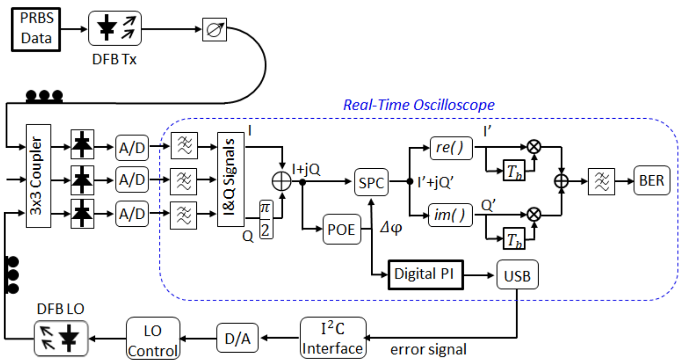

Fig. 2. Experimental setup. Symbol phase correction (SPC) and phase offset estimation (POE) are performed into the DSP stage.

tuning system by simultaneous control on the bias current and the thermoelectric cooler available in the DFB package, with a time constant of 700ns for frequency shifts [11].

VI. Measurements and Results

Initially, the open-loop performance was evaluated. Received optical power was set to -47.5dBm to obtain a reference BER of 10^{-4}. Temperature of Tx DFB laser was adjusted with an external control to sweep the optical frequency. Then, the detected signal was processed to estimate the phase drift $\Delta\varphi$ for different frequency deviations. Numerical simulation was also performed with the same design parameters for comparison. As noticed in Fig. 3, both estimation methods provide a good approximation of a linear estimation for $\Delta\varphi$ in the range Δf = ±500MHz, with zero-crossing when Tx and LO lasers are perfectly matched, suitable for data compensation and LO tuning. In addition, frequency offsets between ±500MHz and ±1.25GHz can be progressively corrected by successive approximations over several feed-back loop periods, as the polarity of the estimated signal remains constant for both algorithms.

In order to test the feed-forward offset compensation, the BER dependence on the frequency offset was measured and plotted in Fig. 4. The intradyne receiver performance without compensation is highly degraded by the frequency offset. On the other hand, compensation of the signal before data recovery and BER calculation exhibits more drift tolerance, with eye opening at 300MHz drift as the insets depict. As expected, for Δf larger than ±500MHz compensation performs worse due to the non-linear characteristic of the estimated phase drift $\Delta\varphi$. In Fig. 5, the BER degradation was translated to a sensitivity penalty for a target BER = 10^{-4}, showing that in the absence of feed-forward compensation the drift tolerance reaches ±100MHz for 1dB power penalty, whereas data detection with offset compensation can tolerate up to ±300MHz for 1dB power penalty, achieving an improvement of 4dB compared to uncompensated detection. It should be also noticed from the test that there is no meaningful difference in the performance between Viterbi and Correlation

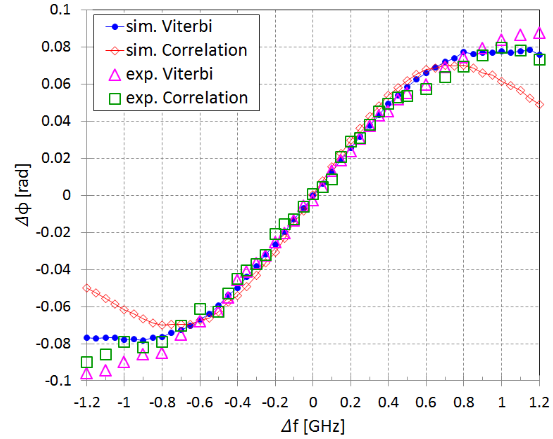

Fig. 3. Simulated (sim.) and experimental (exp.) values for the estimated phase offset vs. frequency drift.

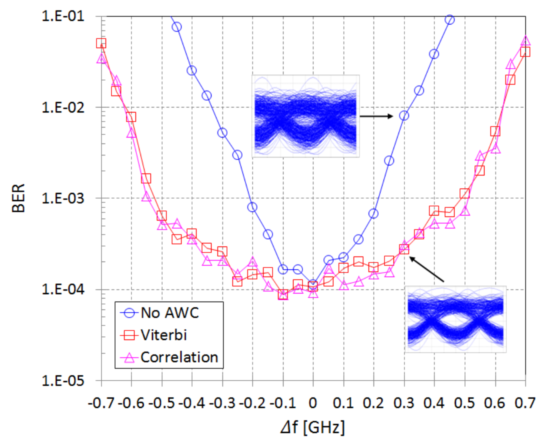

Fig. 4. BER dependence against frequency drift for the intradyne receiver with/out feed-forward data offset compensation, with eye diagram for 300MHz drift.

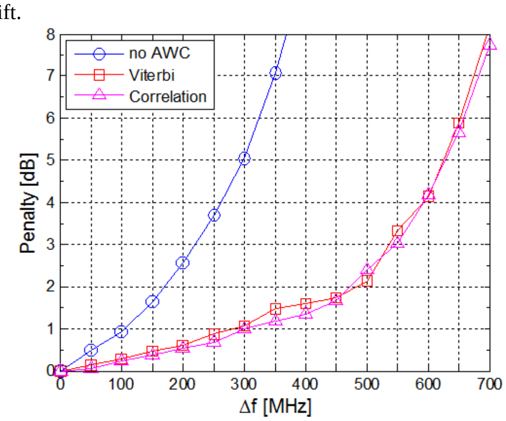

Fig. 5. Sensitivity penalty at BER = 10^{-4} vs. frequency drift for the intradyne receiver with/out feed-forward data offset compensation.

estimation methods.

Next, the dual correction system was tested in closed-loop setup with both feed-back and feed-forward strategies simultaneously. Fig. 6(a) depicts a long-term measurement of frequency offset over 30 minutes for both: free-running Tx and LO lasers physically separated for uncorrelated temperatures, and real-time continuous LO tuning process. It can be noticed

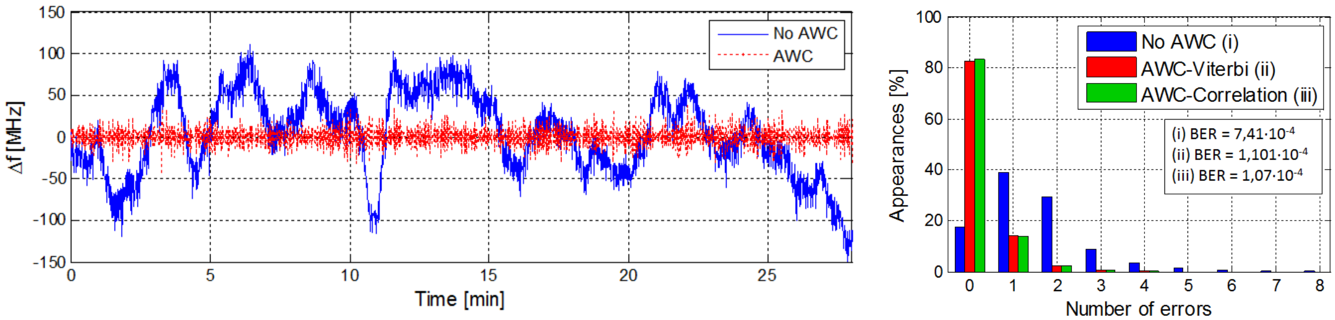

(a) (b)

Fig. 6. Long-term (a) frequency offset measurement and (b) number of errors recorded in frames of 2048 bits at burst-mode operation over 30 minutes test for the intradyne receiver with/out AWC and dual correction stages. The inset represents the measured BER over the 30 min test for the three different scenarios.

that, without any tracking system the IF signal shows a random excursion larger than ±100MHz, due to non-stability of DFB lasers and thermal environmental changes. We also observe that the fastest frequency drift spreads 200MHz in about 55 seconds, leading to a frequency drift rate of 3.6MHz/s, being the LO tuning every 600ms fast enough to correct such frequency drifts. In the udWDM grid, as the channel spacing gets narrower, the tolerable frequency drift becomes more severe, yielding to preclude data detection and to interfere adjacent channels. Such an excursion was suppressed by continuous LO tuning every 600ms. Despite the LO tuning, faster oscillations can be observed, as well as in the case of free-running lasers, due to the phase noise, being later removed from data at the feed-forward compensation stage.

In addition, sequences of 2048 bits were launched in burst-mode on the 30 minutes test, to record the number of errors for each frame. Results, in terms of the percentage of processed frames with a certain number of errors, are plotted in Fig. 6(b). As observed, the AWC with simultaneous strategies accomplishes the target BER = 10^{-4} unchanged over the time, obtaining about 83% of error-free frames for both algorithms.

As a final test, the system was started with an arbitrary 500MHz frequency offset to analyze the dynamics of the real-time LO tuning process, as well as the benefit of the digital PI. According to Fig. 7, by using the PI controller to drive the LO, the frequency offset is corrected in a single loop-time of 600ms with a further reduction of IF oscillations, unlike the AWC system without PI controller.

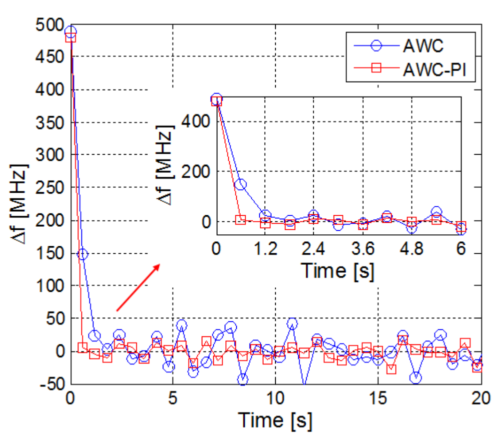

Fig. 7. Real-time closed-loop LO tuning evolution for 500MHz drift.

VII. Conclusion

The AWC for digital coherent receivers with dual correction stages was demonstrated for the first time, with a phase noise tolerance up to a product $\Delta\upsilon T_b = 6.4\cdot10^{-3}$, with common DFB lasers. The two strategies can deal with environmental changes and high laser phase and frequency noise, as the feed-forward stage corrects any residual offset/oscillation after LO tuning. Accurate closed-loop performance at a sensitivity of -47.5dBm for BER = 10^{-4} was achieved with real-time dual correction range as wide as ±500MHz offset in 600ms within 2dB maximum penalty at the sensitivity. This strategy is simple enough to be implemented in a cost-efficient optical network unit for udWDM-PON.

References

[1] S. Savory, "Digital coherent optical receivers: algorithms and subsystems," *J. Selec. Topics in Quant. Elect.*, vol. 16, no. 5, pp. 1164-1179, Sept. 2010.

[2] Z. Tao, H. Zhang, A. Isomura, L. Li, T. Hoshida, J.C. Rasmussen, "Simple, robust, and wide-range frequency offset monitor for automatic frequency control in digital coherent receivers," in *Proc. ECOC*, 2007, paper 3.5.4

[3] J. Prat, V. Polo, P. Zakynthinos, I. Cano, J. Tabares, J.M. Fàbrega, D. Klonidis, I. Tomkos, "Simple intradyne PSK system for udWDM-PON," in *Proc. ECOC*, 2012, paper We.2.B.2

[4] A. Leven, N. Kaneda, U. Koc, Y. Chen, "Frequency estimation in intradyne reception," *IEEE Photon. Technol. Lett*., vol. 19, no. 6, pp. 366-368, 2007.

[5] L. Li, Z. Tao, S. Oda, T. Hoshida, J. Rasmussen, "Wide-range, accurate and simple digital frequency offset compensator for optical coherent receivers," in *Proc. OFC*, 2008, paper OWT4.

[6] M. Roppelt, M. Lawin, M. Eiselt, "Single-fibre operation of a metro access system with network based wavelength control," in *Proc. ECOC*, 2013, paper Tu.3.F.1

[7] F. Natali, "AFC tracking algorithms," *IEEE Trans. Comm.*, vol. 32, no. 8, pp 935-947, 1984.

[8] D. Lavery, R. Maher, D. Milar, B. Thomsen, P. Bayvel, S. Savory, "Digital coherent receivers for long-reach optical access networks" *J. Ligthw. Technol.*, vol. 31, no. 4, pp. 609-620, 2013.

[9] I. Cano, A. Lerín, V. Polo, J. Tabares, J. Prat, "Simple ONU transmitter based on direct-phase modulated DFB laser with heterodyne detection for udWDM-PON," in *Proc. ECOC*, 2013, paper We.2.F.4

[10] C. Xie, P. Winzer, G. Raybon, A. Gnauck, B. Zhu, T. Geisler, B. Edvold, "Colorless coherent receiver using 3x3 coupler hybrids and single-ended detection," *Opt. Exp.*, vol. 20, no. 2, pp 1164-1171, 2012.

[11] V. Polo, P. Borotau, A. Lerín, J. Prat, "DFB laser reallocation by thermal wavelength control for statistical udWDM in PONs," in *Proc. ECOC*, 2014, paper P.4.13.